



*INSTITUT NATIONAL DE RECHERCHE  
SUR LES TRANSPORTS ET LEUR SECURITE*

JF Hamet

## **Reduction of tire road noise by acoustic absorption**

Numerical evaluation of the pass-by noise level reduction using the normal incidence acoustic absorption coefficient

LTE 0423  
October 2004

---

The authors :

Jean-François Hamet  
Directeur de Recherche au Laboratoire Transports et Environnement  
25, avenue François Mitterrand – Case 24, 69675 Bron cedex  
hamet@inrets.fr

## Bibliographic notice

1 Research department (1 <sup>st</sup> author) Laboratoire Transports et Environnement (LTE)		2 Project N° SILVIA (silent roads)	3 INRETS
4 Title Reduction of tire road noise by acoustic absorption			
5 Sub-title Numerical evaluation of the pass-by noise level reduction using the normal incidence acoustic absorption coefficient		6 Language Engl	
7 Author(s) JF Hamet		8 Ext. collaboration	
9 Name, address, financing, co-editor		10 N° contract, conv. GRD2/2000/30202	
		11 Date of publication October 2004	
12 Comments This report is an INRETS-LTE edition of the SILVIA -INRETS-013-WP2 report " <i>Estimation of the attenuation of rolling noise by acoustic absorption</i> ", dated 19/09/2004.			
13 Summary Part of INRETS task in the SILVIA project is to study the influence of the pavement characteristics on the generation and the propagation of road traffic noise using existing models. This work addresses the reduction of tire-road noise by absorption effects. It aims at finding a numerical correspondence between the two quantities generally available from measurements: pass-by noise noise levels at 7.5 m distance and acoustic absorption at normal incidence. Estimations are made using an omnidirectional point source for modeling the tyre, and the image method for modeling the reflection of the porous pavement. The approach is validated by comparing calculations to published experimental results. A numerical correspondence is found between the absorption coefficient in normal incidence and the pass by level difference obtained between a source over the absorbing surface and the source over a reflecting surface. The absorption and attenuation curves in function of frequency have similar shapes but are slightly shifted in frequency. A numerical law is evaluated for standard pass-by measurement conditions (microphone at 7.5 m distance and 1.2 m height). The law is formulated in 1/3 octave values between the frequency shifted absorption coefficient and the attenuation: $\Delta L_p(f_c, 81^\circ) = -11.9 \times \langle a_o(f_{sh.}, 0) \rangle \quad \text{dB}$ The law does not depend on frequency.			
14 Keywords tire road noise, acoustic absorption, noise reduction, measurement, modelling		15 Distribution <b>PUBLIC</b> INRETS/RR/04-537-ENG	
16 Number of pages 25	17 Price	18 Confidential until	19 Bibliography

# Fiche bibliographique

1 UR (1 <sup>er</sup> auteur) Laboratoire Transports et Environnement (LTE)		2 Projet n° SILVIA (silent roads)	3 INRETS
4 Titre Reduction of tire road noise by acoustic absorption			
5 Sous-titre Numerical evaluation of the pass-by noise level reduction using the normal incidence acoustic absorption coefficient		6 Langue Engl	
7 Auteur(s) JF Hamet		8 Rattachement ext.	
9 Nom adresse financeur, co-éditeur		10 N° contrat, conv. GRD2/2000/30202	
		11 Date de publication October 2004	
12 Remarques Ce rapport est l'édition INRETS-LTE du rapport SILVIA -INRETS-011-WP2 " <i>Estimation of the attenuation of rolling noise by acoustic absorption</i> ", publié le 08/08/2003			
13 Résumé <p>Une des contributions de l'INRETS au projet SILVIA est d'évaluer l'influence des caractéristiques de la chaussée sur la génération et la propagation du bruit de trafic routier, en utilisant les modèles existants.</p> <p>Le travail abordé dans ce rapport concerne la réduction du bruit de contact pneumatique-chaussée par absorption acoustique de la chaussée. Il vise à trouver une correspondance numérique entre deux quantités généralement disponibles; le niveau de bruit au passage à 7.5 de distance et le coefficient d'absorption acoustique en onde plane du revêtement, mesuré sous incidence normale.</p> <p>Les évaluations sont effectuées en utilisant pour le rayonnement du pneumatique le modèle d'une source ponctuelle omnidirectionnelle et la méthode des images pour modéliser la réflexion acoustique de la surface du revêtement. L'approche est validé en comparant les calculs aux résultats expérimentaux trouvés dans la littérature.</p> <p>Une correspondance est recherchée entre le coefficient d'absorption acoustique en incidence normale et la différence des niveaux de bruit au passage évaluée entre le cas de la source sur la surface absorbante et celui de la source sur une surface réfléchissante. Les courbes d'absorption acoustique et de réduction de bruit ont des formes similaires mais sont légèrement décalées en fréquence.</p> <p>Une loi numérique est évaluée pour les niveaux de bruit au passage mesurés dans les conditions standard (microphone à 7.5m de distance horizontale et à 1.2m de hauteur). La loi est formulée en 1/3 octave entre le coefficient d'absorption acoustique, décalé en fréquence, et la réduction de niveau de bruit.</p> $\Delta L_p(f_c, 81^\circ) = -11.9 \times \langle a_o(f_{sh.}, 0) \rangle \quad \text{dB}$ <p>La loi est la même pour les 1/3 octave considérés.</p>			
14 Mots-clés Bruit pneumatique chaussée, absorption acoustique, réduction, mesure, modélisation		15 Diffusion libre INRETS/RR/04-537-ENG	
16 Nombres de pages 25	17 Prix	18 Confidentiel jusqu'au	19 Bibliographie

---

# Introduction

---

Acoustic absorption and porosity are two factors reckoned to contribute to traffic noise reduction. Both exist only on porous<sup>1</sup> pavements. Part of the difficulty is to determine their respective contributions: reduction by the porosity of the air pumping generation, reduction by the acoustic absorption of the noise once radiated.

A goal of SILVIA project *Task 2.2 Model application* is to study the influence of the pavement characteristics on the generation and the propagation of road traffic noise using existing models.

This work addresses the reduction of tire-road noise by absorption effects. It aims at finding a numerical correspondence between the two quantities generally available from measurements: pass-by noise levels at 7.5 m distance and acoustic absorption at normal incidence.

Estimations are made using an omnidirectional point source for modeling the tyre, and the image method for modeling the reflection of the porous pavement. The approach is validated by comparing calculations to published experimental results.

A numerical correspondence is found between the absorption coefficient in normal incidence and the pass by level difference obtained between a source over the absorbing surface and the source over a reflecting surface. The absorption and attenuation curves in function of frequency have similar shapes but are slightly shifted in frequency.

A numerical law is evaluated for standard pass-by measurement conditions (microphone at 7.5 m distance and 1.2 m height). The law is formulated in 1/3 octave values between the frequency shifted absorption coefficient and the attenuation:

$$\Delta L_p(f_c, 81^\circ) = -11.9 \times \langle a_o(f_{sh.}, 0) \rangle \quad \text{dB}$$

The law does not depend on frequency.

---

<sup>1</sup>Similar to Sandberg in his tyre/road reference book, the term *porous* is used for facility, although *pervious* would be more appropriate.

---

# Contents

---

<b>1</b>	<b>Experimental observations</b>	<b>6</b>
<b>2</b>	<b>Modeling approach</b>	<b>10</b>
2.1	The model . . . . .	10
2.1.1	Point source over an absorbing surface . . . . .	10
2.1.2	Attenuation by absorption effect . . . . .	11
2.1.3	Acoustic impedance of a multiple layer . . . . .	11
2.1.4	Modeling of the porous medium . . . . .	12
2.2	Experimental validation . . . . .	12
2.2.1	Physical characteristics determined from the absorption measurements	12
2.2.2	Physical characteristics adjusted to the attenuation values . . . . .	12
<b>3</b>	<b>Parametric study</b>	<b>15</b>
3.1	Influence of the geometry . . . . .	15
3.2	Influence of the physical characteristics . . . . .	17
3.2.1	Layer thickness . . . . .	17
3.2.2	Tortuosity of the porous medium . . . . .	17
3.2.3	Porosity of the porous medium . . . . .	17
<b>4</b>	<b>Acoustic absorption and noise attenuation</b>	<b>19</b>
4.1	Acoustic absorption for plane waves and spherical waves . . . . .	19
4.2	Reflection coefficient and noise reduction . . . . .	20
4.3	Absorption coefficient and noise reduction . . . . .	20
4.4	Estimating $\Delta L_{PB}$ from $a_o$ . . . . .	21
4.5	Example . . . . .	23
<b>5</b>	<b>Conclusion</b>	<b>24</b>
	<b>Bibliography</b>	<b>25</b>

---

# 1 – Experimental observations

---

Tire road noise is generally seen to decrease with texture depth. On very smooth surfaces however tire road noise may increase when texture depth decreases (Fig. 1.1). On standard surfaces, a decrease of road roughness results in a decrease of tire vibrations and consequently in noise. On very smooth surfaces a *sealing effect* occurs between the road and the tire surface as the road gets smoother [1]: air pumping phenomena occur.

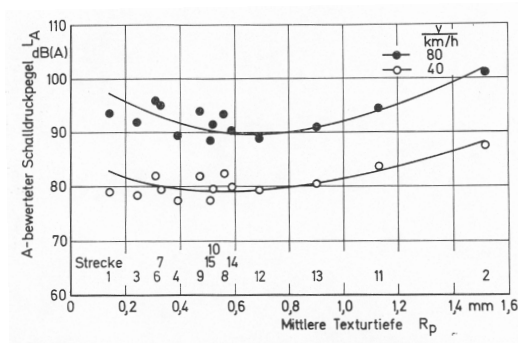


Figure 1.1: Relation between the noise level  $L_A$  of a tire rolling at 40 km/h and 80 km/h on dry surfaces and the mean texture depth  $R_p$  of these surfaces (from [2])

Porosity strongly reduces air pumping noise. Porous pavements also have acoustic absorption properties and consequently acoustic attenuation properties. This was already reckoned in the 70's: *tread-cavity pressure difference can be neutralized through the surface porosity [...] Porosity results in better sound absorption properties.* [1]

**Sandberg and Descornet [3]** observed in the late 70's that the measured tire road noise level difference between an acoustically absorbing surface and a perfectly reflecting surface was higher than the measured difference on sound propagation over these surfaces<sup>1</sup>

**Oshino [4]** more recently measured the tire/road noise over three surfaces: a dense asphalt pavement and two porous pavements. He also measured the attenuation due to sound absorption for a source placed at each tire and engine position, including multiple reflection under the car body (Fig 1.2).

By removing the absorption effect from the pass-by results on the drainage pavements (Fig 1.3 zone A) he estimated the noise reduction due to porosity (Fig 1.3 zone B ).

---

<sup>1</sup>The two surfaces were considered to have "similar" texture spectra

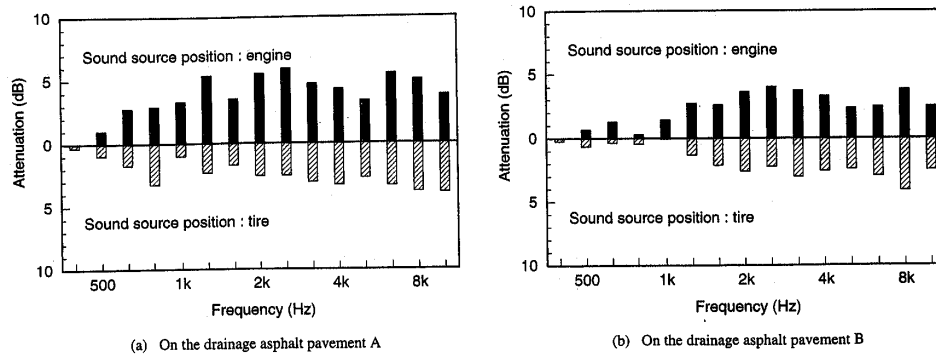


Figure 1.2: attenuation due to sound absorption during multiple reflection (passenger car) (from [4]).

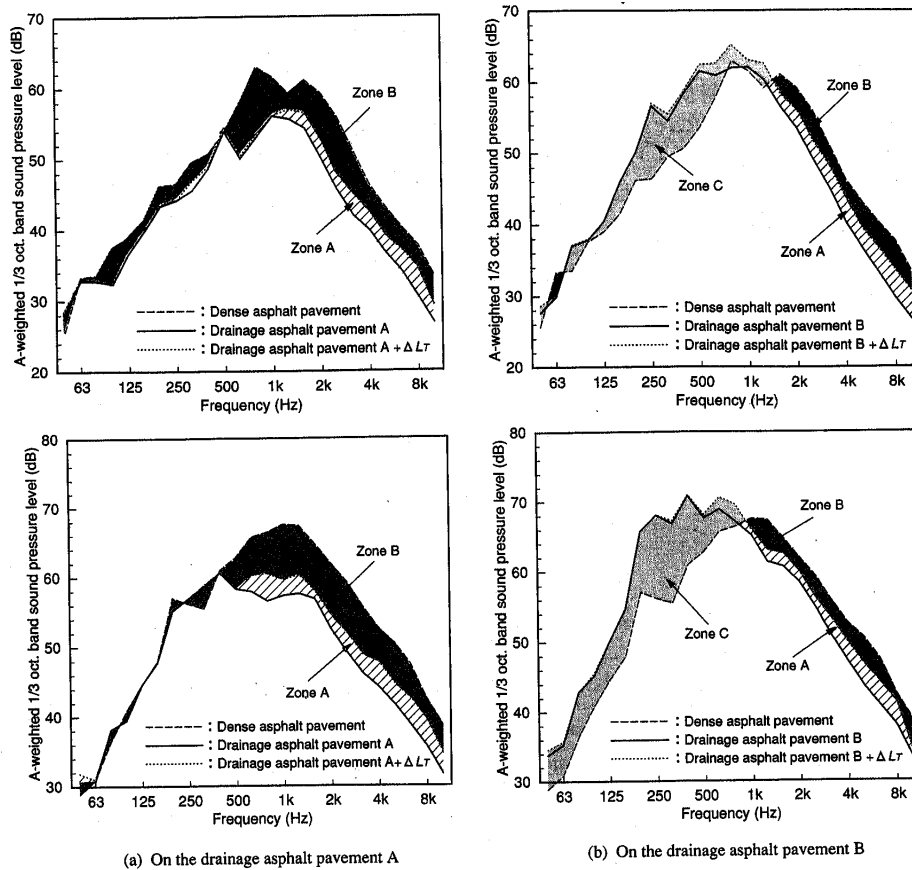


Figure 1.3: Tire/road noise on a drainage asphalt pavement and on a dense asphalt pavement.

Top: passenger car, 60 km/h - Bottom: heavy truck, 60 km/h.

Zone A: sound reduction effect due to sound absorption.

The curve  $A + \Delta LT$  is the expected tire/road noise level with the absorption effect suppressed. (from [4]).

**”Proefvak Welschap” experiment [5]** In the 90’s controlled pass-by measurements were performed in the frame of the Dutch research project ”Proefvak Welschap”. Pass by 1/3 octave levels were evaluated at 60 km/h and 120 km/h (Fig 1.4).

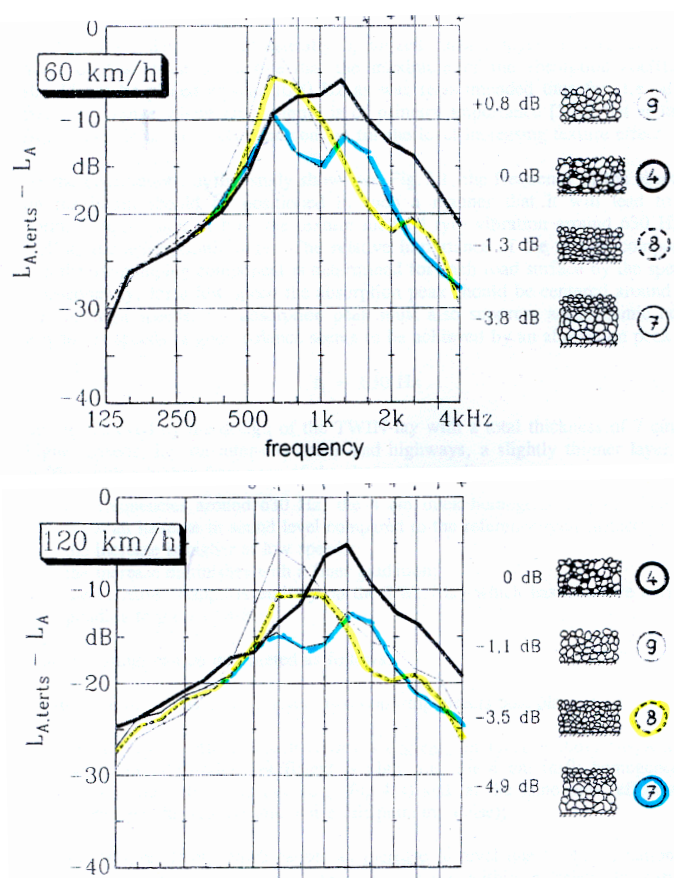


Figure 1.4: 1/3 octave spectra of porous surfaces relative to the reference surface N°4 (0 dB)  
From [5]

Two porous surfaces turn out to have the same type of rolling course (porous layer with 4/8 grading): one is a single layer 4 cm thick, the other a double layer (lower layer: 11/16 grading, 4.5 cm thick; upper layer: 4/8 grading, 2.5 cm thick).

It can thus be expected that the tire noise generation (vibration and air pumping) is the same on both surfaces and that pass-by noise level differences should be due to differences in the acoustic absorption properties of the pavements.

The measured level differences are given Table 1.1. They depend little on speed. At low frequencies both surfaces yield the same tire road noise as expected. The double layer becomes ”quieter” than the single layer in the octave 800 Hz, ”noisier” in the octave 1600 Hz, quieter again in the octave 3200 Hz (Fig 1.4).

km/h	500	630	800	1000	1250	1600	2000	2500	3150	4000
60	-2	-4	-7	-5	+3	+5.5	+2.5	-3	-2.5	+2
120	0	-4	-5.5	-5	+2	+5	+2	-2	-1	+2

Table 1.1: sound level differences between track 7 (double layer) and track 8 (single layer). The differences were read from Fig 1.4.

The acoustic absorption was measured on cores, in normal incidence using a stationary wave tube. Results are drawn Fig 1.5. The absorption coefficient of the single layer is maximum at 1040 Hz while it is maximum at 550 Hz for the double layer.

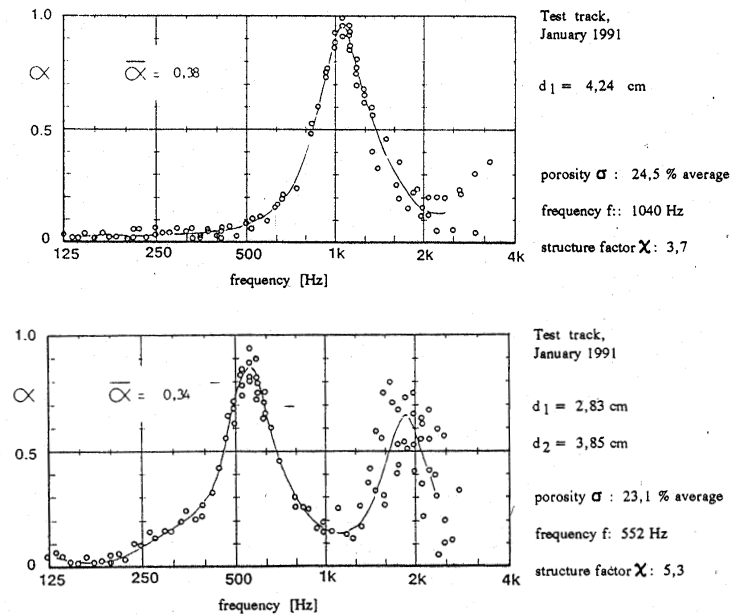


Figure 1.5: Acoustic absorption coefficient in normal incidence.  
Top: single layer. Bottom: double layer. From [5]

As expected qualitatively, each porous layer turns out to be quieter than the other when its acoustic absorption is higher: there is some correspondence between sound absorption and tire noise reduction.

---

## 2 – Modeling approach

---

The tire source is modeled by an omnidirectional point source. This is a great simplification of the phenomena at stake. It may nevertheless give relevant information regarding noise attenuation over absorbing surfaces. It will be checked later on by comparing the results to those obtained using another model which takes into account the noise radiated by a vibrating tyre over an absorbing surface.

### 2.1 The model

#### 2.1.1 Point source over an absorbing surface

The geometry of the problem is given Fig 2.1: the acoustic pressure field created by the point source over the surface is made of a direct field and a reflected field. The reflected field is obtained using an image method<sup>1</sup>: the acoustic reflection is formulated using a reflection coefficient  $Q(f, \theta)$ . The pressure level  $L_p$  is written

$$L_p(f) = L_w(f) - 10 * \log(4\pi r_s^2) + 20 * \log \left| 1 + \frac{r_i}{r_s} Q(f, \theta) e^{ik\Delta r} \right| \quad (2.1)$$

with  $L_w(f)$  the acoustic power of the source at frequency  $f$ ,  $\Delta r = |r_i - r_s|$ .

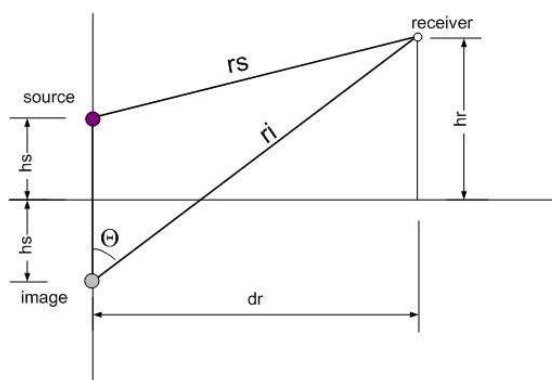


Figure 2.1: Geometry of source and receiver

The reflection coefficient<sup>2</sup>  $Q(f, \theta)$  is expressed in terms of the plane wave reflection

<sup>1</sup>The principle, easily justified for a reflection by a porous half space, has been "heuristically" extended to reflection by single or multiple layers [6]. The validity of this extension will eventually be addressed in another report.

<sup>2</sup> $Q$  depends on several factors as can be seen in Eq 2.2; we write  $Q(f, \theta)$  to stress the dependency on frequency and angle of "incidence", similarly for  $R_p(f, \theta)$

coefficient  $R_p(f, \theta)$  (cf. for instance [7, 8]):

$$\begin{aligned} Q(f, \theta) &= R_p(f, \theta) + [1 - R_p(f, \theta)] F(w) \\ F(w) &= 1 + i\pi^{1/2} w e^{-w^2} \operatorname{erfc}(-iw) \\ w &= \frac{1+i}{2} (k_o r_i)^{1/2} [\cos \theta + \rho_o c_o / Z(f, \theta)] \end{aligned} \quad (2.2)$$

$$R_p(f, \theta) = \frac{\cos \theta - \rho_o c_o / Z(f, \theta)}{\cos \theta + \rho_o c_o / Z(f, \theta)} \quad (2.3)$$

$\rho_o c_o$  the air impedance,  $\theta$  the angle with respect to the surface normal,  $Z(f, \theta)$  the surface impedance for plane-wave,  $k_o = 2\pi f / c_o$  the wave number in air,  $r_i$  the distance between the the image source and the receiver (Fig 2.1).

### 2.1.2 Attenuation by absorption effect

The acoustic absorption effect of the pavement will be characterized by the difference  $\Delta L_{PB}$  in pass-by maximum sound pressure level between what is observed over the absorbing surface ( $0 < Q < 1$ ) and what is observed over a perfectly reflecting surface ( $Q = 1$ ). For the point source model it is :

$$\Delta L_{PB}(f) = 20 \log \left| 1 + \frac{r_i}{r_s} Q(f, \theta) e^{ik\Delta r} \right| - 20 \log \left| 1 + \frac{r_i}{r_s} e^{ik\Delta r} \right| \quad (2.4)$$

Tyre noise radiation is reckoned to be most important in the vicinity of the contact zone, the source will thus be placed on the surface, i.e.  $h_s = 0$ . Consequently  $r_i = r_s$  and  $\Delta r = 0$ .

The estimation of the pass-by tyre noise level reduction is then given by the expression

$$\Delta L_{PB}(f, \theta) = 20 \log [|1 + Q(f, \theta)| / 2] \quad (2.5)$$

When  $Q = 1$  (full reflection),  $\Delta L_{PB} = 0$ , there is no difference in the pass-by levels (both surfaces are fully reflecting); when  $Q = 0$  (full absorption) the pass-by level over the absorbing surface differs by  $\Delta L_{PB} = -6$  dB from the one over the perfectly reflecting surface.

### 2.1.3 Acoustic impedance of a multiple layer

The attenuation by acoustic absorption depends on the reflection coefficient  $Q(f, \theta)$ , which itself depends on the geometry ( $\theta$  and  $r_i$ ) and on the acoustic impedance  $Z(f, \theta)$  of the surface.

For the general case of a multiple layer, the acoustic impedance is obtained by iteration starting from the lower layer [9]: the 'top' impedance  $Z$  of each successive layer is given by

$$Z = W \frac{W + Z_B \coth \gamma e}{Z_B + W \coth \gamma e} \quad (2.6)$$

where  $Z_B$  and  $e$  are the 'backing' impedance and the thickness of the layer,  $W$  and  $\gamma$  its specific acoustic impedance and propagation constant given by<sup>3</sup>:

$$W = \frac{\rho c}{\mu} \quad \gamma = i \frac{\omega}{c} \mu \quad \mu = \sqrt{1 - \frac{c_o^2}{c^2} \sin^2 \theta} \quad (2.7)$$

$\rho$  and  $c$  are the complex density and celerity of the layer medium. The expressions take into account the oblique incidence throughout the quantity  $\mu$  ([6, 9] for instance).

<sup>3</sup>The convention  $e^{i\omega t}$  is used here

### 2.1.4 Modeling of the porous medium

The modelling used here for porous media is the phenomenological model [10,11]: a porous medium is characterized by three physical parameters: its specific airflow resistance  $R_s$ , porosity<sup>4</sup>  $\Omega$ , and tortuosity  $K$ . The complex density and celerity of the medium are given by

$$\rho = \rho_o \frac{K}{\Omega} [1 - i f_\mu / f] \quad c = c_o \frac{1}{\sqrt{K}} [1 - i f_\mu / f]^{-1/2} \left[ 1 + \frac{\gamma_p - 1}{1 + i f / f_\theta} \right]^{-1/2} \quad (2.8)$$

$$f_\mu = \frac{1}{2\pi} \frac{R_s}{\rho_o} \frac{\Omega}{K} \quad f_\theta = \frac{1}{2\pi} \frac{1}{N_{pr}} \frac{R_s}{\rho_o} \quad (2.9)$$

$\gamma_p = 1.4$  and  $N_{pr} = 0.71$  are the specific heat ratio and Prandtl number for air.

## 2.2 Experimental validation

In the "Proefvak Welschap" experiment the pass-by noise levels were measured with a microphone at 5 m height [5]

$h_s$	$h_r$	$d_r$	$\theta$
0	5 m	7.5 m	56°

Table 2.1: Geometry used for the for the experiment [5].

### 2.2.1 Physical characteristics determined from the absorption measurements

The physical characteristics of the two layers are estimated from the absorption values (Fig 1.5), the results are given Table 2.2. For the estimation it is assumed that the

	$e$ [cm]	$R_s$ [kNs/m <sup>3</sup> ]	$\Omega$	$K$
single layer	4.24	25.8	0.20	2.6
double: upper layer	2.83	25.8	0.20	2.6
double: lower layer	3.85	21.0	0.24	5

Table 2.2: Physical characteristics estimated from measured absorption values (Fig1.5)

characteristics of the double layer rolling course (upper layer) are the same that those of the single layer. Calculated and measured absorption values are drawn Fig 2.2.

The estimated  $\Delta L_{PB}$  values of the two porous pavements, are drawn Fig 2.3 (graph to the left). The corresponding difference between the pavements  $\Delta L_{PB,double} - \Delta L_{PB,single}$  is drawn on the graph to the right together with the experimental values. The calculated values seem somewhat shifted w.r.t. the experimental values.

### 2.2.2 Physical characteristics adjusted to the attenuation values

The observed differences may be due various causes: too simple a modeling, erroneous values for the characteristics, etc. The objective of this work is not to reconstitute the reality but to check whether a simple model can give a satisfactory estimation of this reality.

<sup>4</sup>air filled pores connected to the upper surface

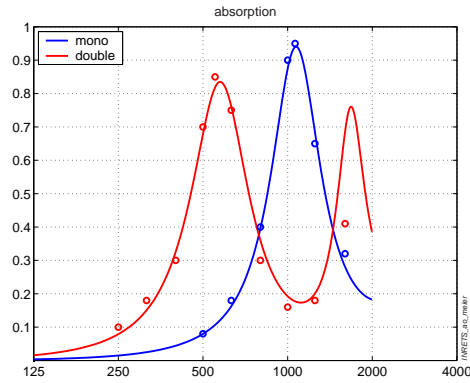


Figure 2.2: Normal incidence absorption coefficient of the single and double layer. Lines: using values from Table 2.2. Circles: experimental values

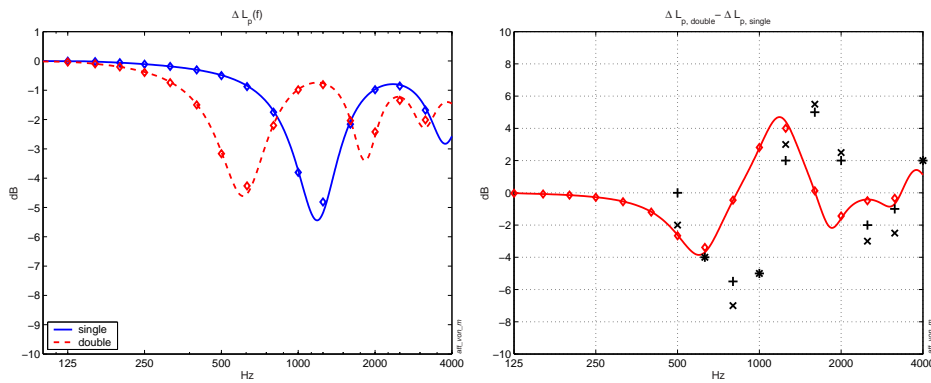


Figure 2.3: Left:  $\Delta L_{PB}(f)$  of the single and the double layer pavements. Right: resulting pass-by noise level differences between the two pavements - The calculations (lines and circles) are made using Table 2.2 values. The experimental values are those of Table 1.1.

Changing the thickness of the layers as indicated Table 2.3 improves the correspondence between measured and calculated attenuations<sup>5</sup> (Figure 2.4, graph to the right) but degrades the correspondence between the absorption coefficients (Fig 2.5).

**Conclusion** Despite these discrepancies it appears that the pass-by noise level differences between these two porous pavements<sup>6</sup> can be explained by a difference in their acoustic absorption properties. The pass-by level difference can reasonably be estimated using the simple omnidirectional point source model.

<sup>5</sup>There may be other combinations which yield a good fit.

<sup>6</sup>which have a same surface texture

	$e$ [cm]	$Rs$ [kNs/m <sup>3</sup> ]	$\Omega$	$K$
single layer	<b>3.0</b>	25.8	0.20	2.6
double: upper layer	<b>2</b>	25.8	0.20	2.6
double: lower layer	<b>3.0</b>	21.0	0.24	5

Table 2.3: Physical characteristics fitted for the excess attenuation (Fig 2.4)

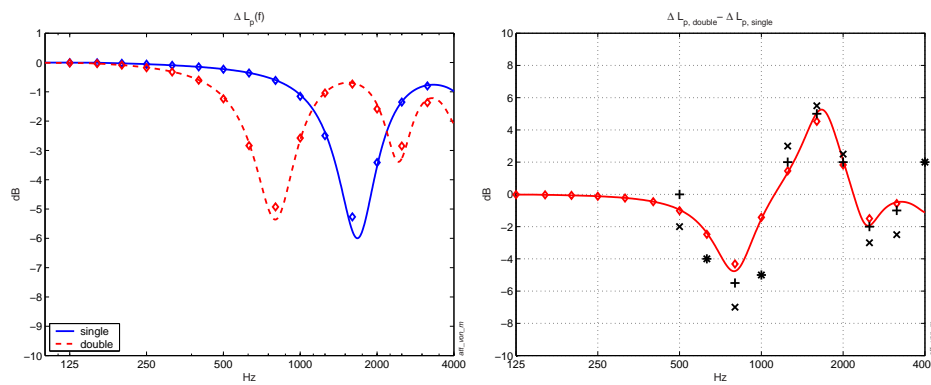
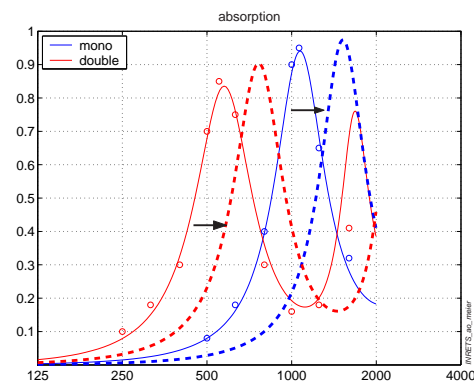
Figure 2.4: Left:  $\Delta L_{PB}(f)$  of the single and the double layer pavements. Right: resulting difference between the two pavements. - The calculations (lines and circles) are made using Table 2.3 values. The experimental values are those of Table 1.1.

Figure 2.5: Absorption coefficient in normal incidence. Full line: adjusted to absorption measurements (Table 2.2). Dotted line : adjusted to attenuation (Table 2.3).

---

## 3 – Parametric study

---

The pass-by noise levels of the "Proefvak Welschap" experiment were measured with a microphone at a height  $h_r = 5$  m while the standard height for this kind of measurements is  $h_r = 1.2$  m. For the modeling, the source was positioned on the ground surface: ( $h_s = 0$  m) while it is rather considered to be at about 1 cm to 5 cm height [12].

Questions thus raise regarding the absorption effect observed at a standard microphone height, the sensitivity of the results to the source height, etc. These points are addressed through a parametric study. Evaluations will be made for deviations from a standard situation. The references will be a single porous layer with characteristics of Table 3.1 and the standard pass-by measurement geometry as given Table 3.2.

$e$	$Rs$	$\Omega$	$K$
4 cm	20 kNs/m <sup>3</sup>	0.20	4

Table 3.1: Characteristics of the reference layer

$h_s$	$h_r$	$d_r$	$\theta$
0	1.2 m	7.5 m	81°

Table 3.2: Standard geometry conditions

The plane wave absorption coefficient of the layer at normal incidence is drawn Figure 3.1.

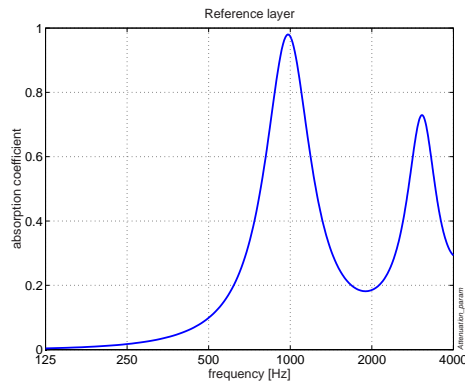


Figure 3.1: Plane wave absorption coefficient at normal incidence of the reference layer

### 3.1 Influence of the geometry

#### Microphone height

As indicated, the pass-by levels of the "Proefvak Welschap" experiment were measured with a microphone at a height  $h_r = 5$  m. The motivation of the authors was that the

acoustic effect of the absorbing surfaces would be reduced. The modeling confirms this hypothesis: the reduction for  $h_r = 1.2$  m is more important than for  $h_r = 5$  m (Figure 3.2).

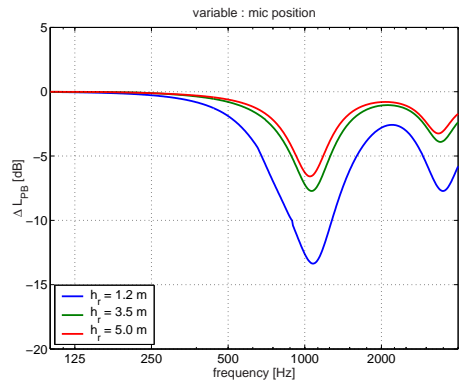


Figure 3.2: Influence of the microphone height

Choosing  $h_r = 3$  m instead of  $h_r = 5$  m does not change much the results.

### Source height

For a microphone at  $h_r = 1.2$  m height,  $\Delta L_{PB}$  does not vary much when the source height changes from 1 cm to 4 cm or 8 cm (Figure 3.3 graph to the left).

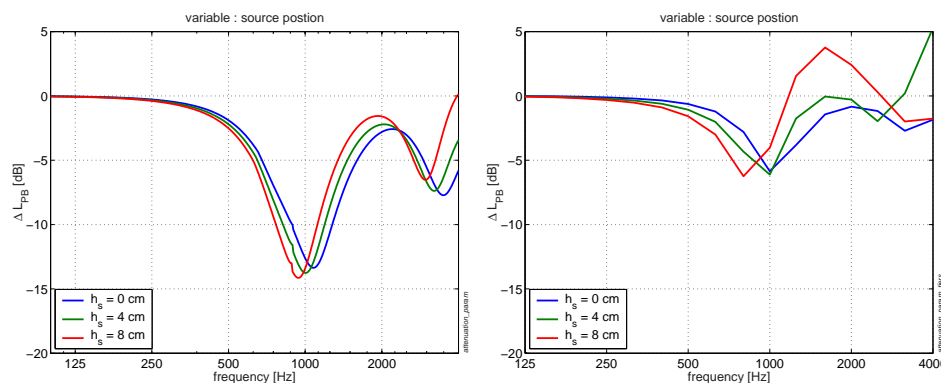


Figure 3.3: Influence of the source height. Left: with  $h_r = 1.2$  m. Right: with  $h_r = 5.0$  m.

The situation is not the same for a microphone at  $h_r = 5$  m: pronounced interferences occur in the high frequency range, creating large differences in a narrow frequency range. The results are thus given in 1/3 bands<sup>1</sup> to smooth out the interference effects.

The results obtained with a source at  $h_s = 4$  cm are close to those obtained with a source on the surface. With a source at  $h_s = 8$  cm the interference ( $k\Delta r = \pi$ ) occurs within the considered frequency range (around 2000 Hz); in the neighborhood of the interference the reflecting surface appears less noisy than the absorbing surface<sup>2</sup>.

### Horizontal distance

A deviation of 50 cm from the  $d_r = 7.5$  m standard value has little effect on the attenuation.

<sup>1</sup>i.e. taking for  $\Delta L_{PB}$  1/3 differences between 1/3 octave levels, not differences between levels at the central frequencies.

<sup>2</sup>For  $h_r = 1.2$  m the interference occurs beyond 6000 Hz.

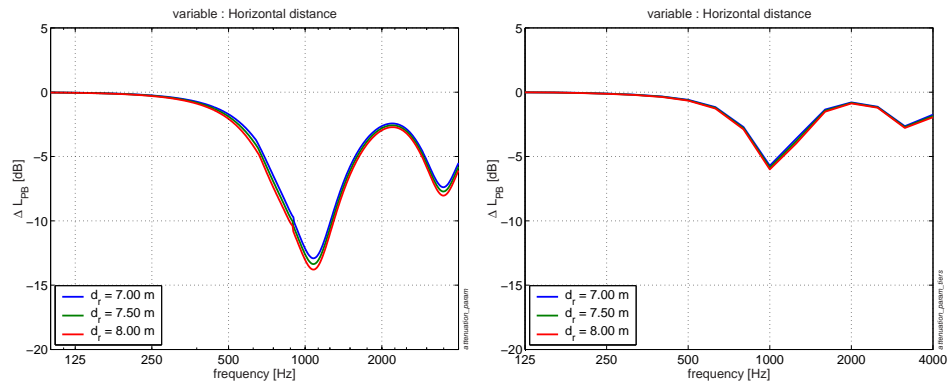


Figure 3.4: Influence of the horizontal distance. Left:  $h_r = 1.2$  m. Right:  $h_r = 5.0$  m.

## 3.2 Influence of the physical characteristics

In this part the term 'acoustic absorption' in the figure captions refers to the plane wave acoustic absorption coefficient at normal incidence.

### 3.2.1 Layer thickness

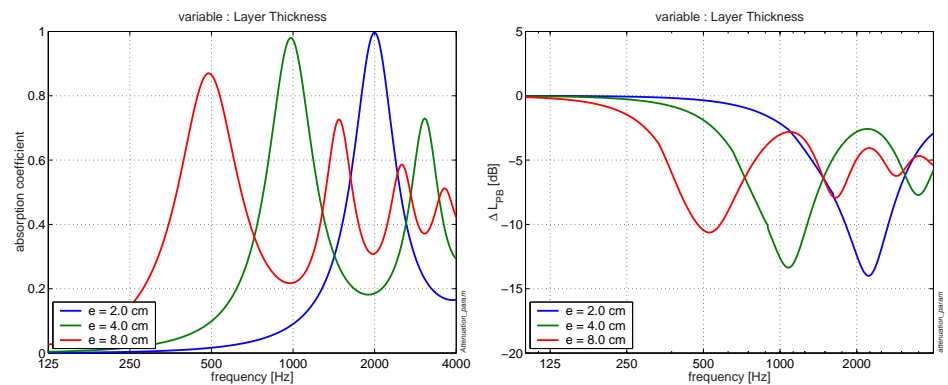


Figure 3.5: Influence of the layer thickness. Left: acoustic absorption. - Right: attenuation  $\Delta L_{PB}$

The evolution of  $\Delta L_{PB}$  somewhat follows the evolution of the acoustic absorption, particularly regarding the shift of the frequencies at which minimum attenuation/ maximum absorption occur.

### 3.2.2 Tortuosity of the porous medium

Same comments as above, except that the tortuosity has little effect on the maximum absorption while it changes the minimum attenuation.

### 3.2.3 Porosity of the porous medium

The porosity widens the zone of the extremum.

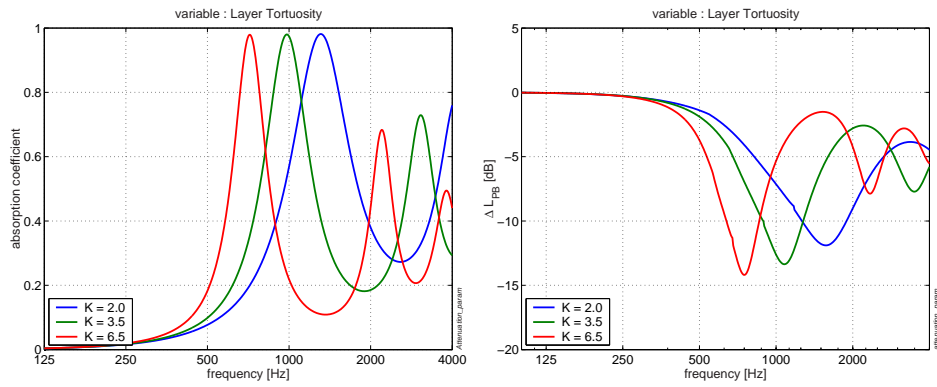


Figure 3.6: Influence of the layer tortuosity.  
Left: acoustic absorption. - Right: attenuation  $\Delta L_{PB}$

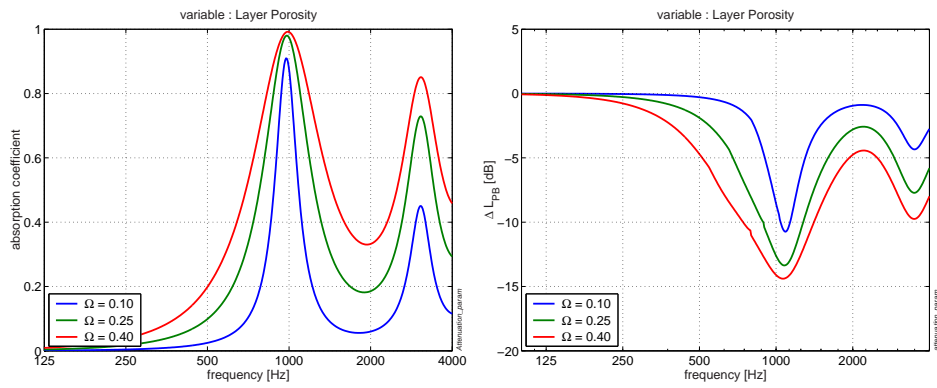


Figure 3.7: Influence of the layer porosity.  
Left: acoustic absorption. - Right: attenuation  $\Delta L_{PB}$

## 4 – Acoustic absorption and noise attenuation

In the parametric study, sound attenuation and acoustic absorption appeared to be in strong correspondence. A priori it does not have to be so:

- the acoustic absorption deals with energy values,  $1 - |R_p|^2$  for plane waves  $1 - |Q|^2$  for spherical waves, while the attenuation deals with modulus and phase values:  $20 * \log |1 + R_p|$  for the plane waves,  $20 * \log |1 + Q|$  for the spherical waves,
- the observed correspondence occurs between the plane wave acoustic absorption in normal incidence  $1 - |R_p(f, 0^\circ)|^2$  and the spherical wave attenuation at quite oblique incidence  $20 * \log |1 + Q(f, 81^\circ)|$  for the standard pass-by geometry.

These points will be addressed in this chapter.

The absorbing layer and the geometry conditions used for the numerical evaluations are the standards of the preceding chapter (Tables 3.1 and 3.2).

### 4.1 Acoustic absorption for plane waves and spherical waves

The acoustic absorption coefficients  $1 - |R_p|^2$  for plane waves  $1 - |Q|^2$  for spherical waves are drawn Figure 4.2 in normal incidence condition (graph to the left) and oblique incidence condition (graph to the right).

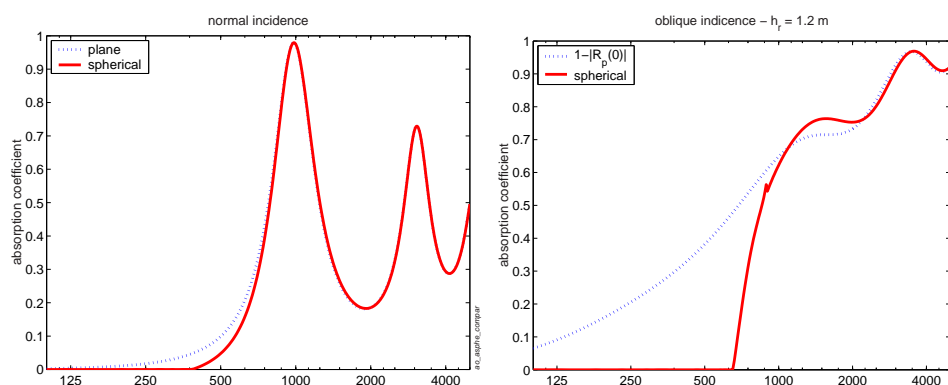


Figure 4.1: Plane-wave and spherical-wave absorption coefficients. Left: normal incidence. Right:  $\theta = 81^\circ$

The absorbing properties of the pavement in normal and oblique incidence are quite different:

- At normal incidence (left graph), high values are observed in narrow frequency ranges ( $\sim 100$  Hz and 3000 Hz)
- At oblique incidence, with here a rather high angle with respect to the normal ( $\theta \sim 81^\circ$ ), the absorption is important from 1000 Hz on.

As expected the coefficients at normal incidence are close. At oblique incidence differences are mainly observed in the low frequency range.

## 4.2 Reflection coefficient and noise reduction

The noise reduction  $\Delta L_{PB} = 20 * \log(|1 + Q(f, \theta)|/2)$  can be estimated using the plane wave reflection coefficient, i.e. by the quantity  $20 * \log(|1 + R_p(f, \theta)|/2)$ , provided the evaluation is made at the actual angle of incidence (Figure 4.2 graph to the right).

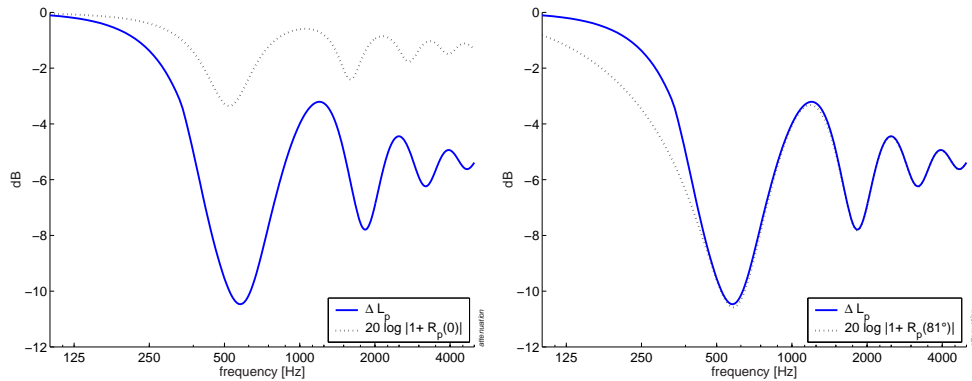


Figure 4.2: Noise reduction  $\Delta L_{PB}(f, 81^\circ)$  and estimation  $20 * \log(|1 + R_p|/2)$ . Left:  $R_p(f, 0)$ . Right:  $R_p(f, 81^\circ)$

The estimation cannot be made using the normal incidence plane wave reflection coefficient  $R_p(f, 0)$ : the result is erroneous (Figure 4.2 graph to the left).

## 4.3 Absorption coefficient and noise reduction

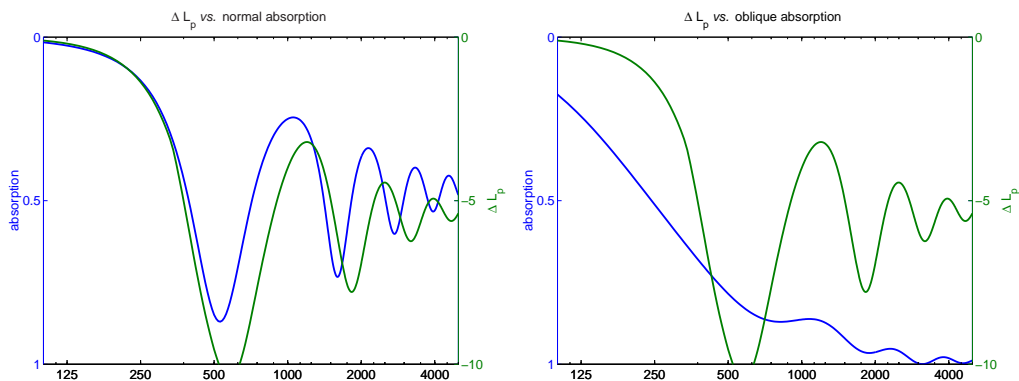


Figure 4.3: Noise reduction  $\Delta L_{PB}(f, 81^\circ)$  and plane wave absorption coefficient  $a = 1 - |R_p|^2$ . Left: normal incidence absorption coefficient  $a_o(f)$ . Right: oblique ( $\theta = 81^\circ$ ) incidence absorption coefficient  $a_{81}(f)$

A strong correspondence is observed between the plane wave (energetic) absorption coefficient  $a$  and the pass-by noise level reduction  $\Delta L_{PB}$ , but strangely enough, this correspondence occurs between the normal incidence absorption coefficient  $a_o(f)$  and the oblique incidence pass-by noise reduction  $\Delta L_{PB}(f, 81^\circ)$  (Figure 4.3 graph to the left). The reason of this will not be addressed in this report.

## 4.4 Estimating $\Delta L_{PB}$ from $a_o$

The following conventions are used:

$$\langle a_o(f_c) \rangle \equiv \frac{1}{\Delta f_c} \int_{f_{cinf}}^{f_{csup}} a_o(f) df = \frac{1}{\Delta f_c} \int_{f_{cinf}}^{f_{csup}} [1 - |R_p(f, 0)|^2] df \quad (4.1)$$

$$\Delta L_{PB}(f_c, \theta) = 10 \log \frac{E(f_c, Q)}{E(f_c, 1)} \quad (4.2)$$

$$E(f_c, Q) = \int_{f_{cinf}}^{f_{csup}} |1 + Q(f, \theta)|^2 df \quad (4.3)$$

$\langle a_o(f_c) \rangle$  is the average of the acoustic absorption coefficient in normal incidence, taken over the 1/3 octave bandwidth (central frequency  $f_c$ , frequency bandwidth  $\Delta f_c = f_{csup} - f_{cinf}$ ).

A set of values  $\{\langle a_o \rangle, \Delta L_{PB}\}$  is used to evaluate the correspondence between the acoustic absorption and the pass-by noise level reduction. It is created by considering a single porous layer and by changing its characteristics (within realistic ranges of values).

### Relation between $\Delta L_{PB}$ and $\langle a_o(f_{sh}) \rangle$ in each 1/3 octave

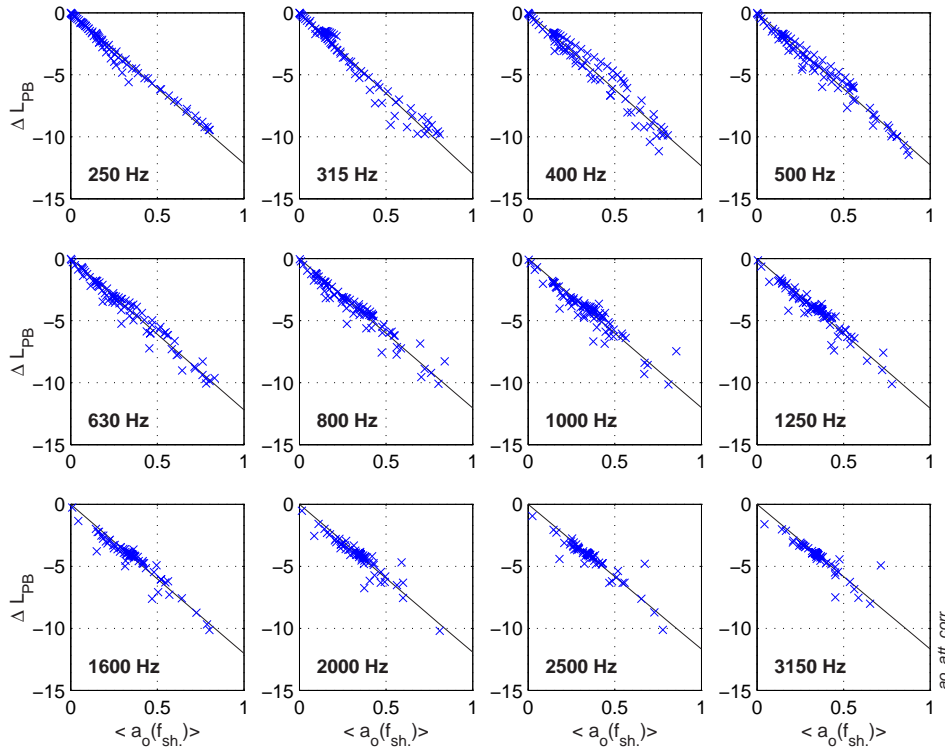


Figure 4.4: Relation between  $\langle a_o(f_{sh}) \rangle$  and  $\Delta L_{PB}$

It can be observed in the parametric study that the  $a_o(f)$  and  $\Delta L_{PB}(f, 81^\circ)$  curves are slightly shifted in frequency (see also Figure 4.3, graph to the left). This is taken into account in the numerical evaluation by frequency shifting the  $a_o$  curve. The third octave  $a_o$  mean value for the frequency band with central frequency  $f_c$  expressed in terms of the

shifting coefficient  $C$  is

$$\langle a_o(f_{sh}) \rangle = \frac{1}{\Delta f_c} \int_{f_{cinf}}^{f_{csup}} a_o(f/C) df \quad (4.4)$$

The  $\{\langle a_o(f_{sh}) \rangle, \Delta L_{PB}\}$  correspondence is found to be best for  $C = 0.91$ . This case is drawn Figure 4.4. It is seen to be indeed very strong, and somewhat independent of frequency.

In the remaining  $\langle a_o(f_{sh}) \rangle$  will implicitly mean  $C = 0.91$

### Relation between $\Delta L_{PB}$ and $\langle a_o(f_{sh}) \rangle$ independently of frequency

Plotting the whole set  $\{\langle a_o(f_{sh}) \rangle, \Delta L_{PB}(f_c, 81^\circ)\}$  on a single graph (Figure 4.5, graph to the left) yields a satisfactory correspondence.

The regression law is found to be:

$$\Delta L_{PB}(f_c, 81^\circ) = -11.9 \times \langle a_o(f_{sh}) \rangle \quad \text{dB} \quad (4.5)$$

**Remark** If a correspondence is looked for between the attenuation  $\Delta L_{PB}(f_c, 81^\circ)$  and the usual absorption coefficient  $a_o(f_c)$  in normal incidence, the result is less satisfactory (Figure 4.5, graph to the right) although the same trend remains.

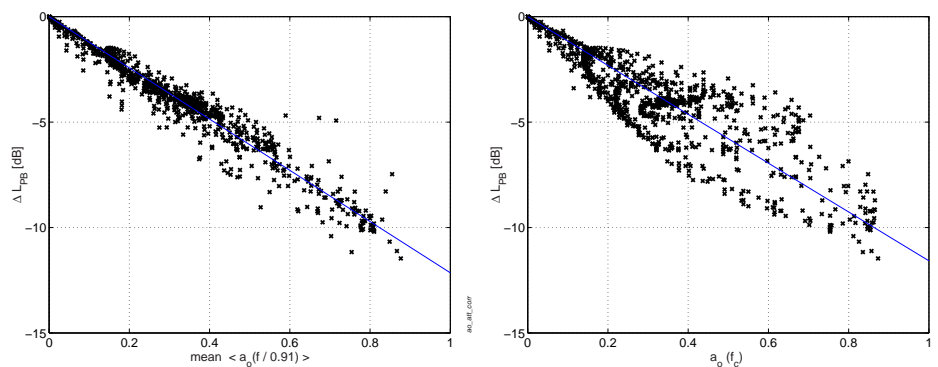


Figure 4.5: Relation between  $a_o$  and  $\Delta L_{PB}$  - Left: using the mean of the frequency shifted coefficient:  $\langle a_o(f_{sh}) \rangle$  - Right: using the standard absorption coefficient:  $a_o(f_c)$

## 4.5 Example

Two estimations obtained using Eq 4.5 are illustrated Figure 4.6. The graph on the left is obtained on the standard single layer (characteristics of Table 3.1), the graph to the right is obtained on a layer twice as thick.

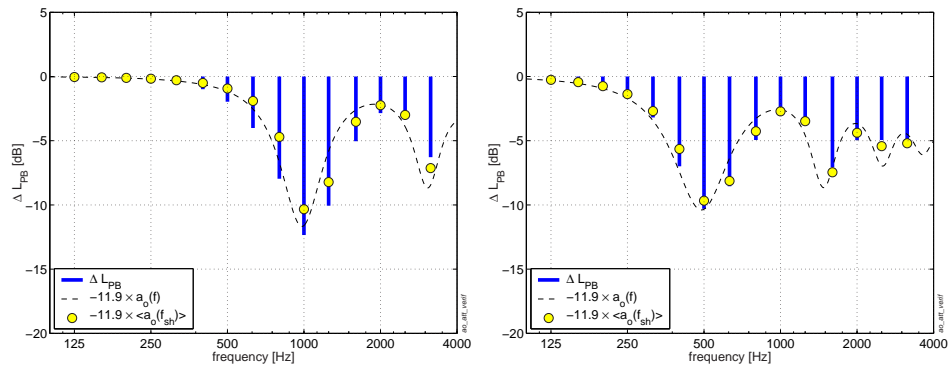


Figure 4.6:  $\Delta L_{PB}$  (blue bars) and its estimations. Yellow circles:  $-11.9 \times \langle a_o(f_{sh}, 0) \rangle$   
 - Dotted curve :  $-11.9 \times a_o(f_c)$   
 Left: standard layer 4 cm thick. Right: layer 8 cm thick

The numerical estimation of  $\Delta L_{PB}$  using Eq 4.5 (yellow circles on the graph) is rather satisfactory considering the simplicity of the formula. For these two examples, the even more simple estimation  $\Delta L_{PB} = -11.9 \times a_o(f_c)$  appears to be also acceptable (dotted curve on the graphs).

---

## 5 – Conclusion

---

The pass-by noise reduction observed on porous surfaces as compared to impervious surfaces (*ceteris paribus*) is attributed to two factors: a decrease of the air pumping noise generation due to porosity effect, a reduction of the radiated noise due to absorption and propagation effects. The study addresses the reduction of the radiated noise and focuses on tyre/ road noise.

The tyre/road source is modeled by a simple omnidirectional point source placed directly on the surface. This is a great simplification of the source. The results will deserve to be compared to evaluations obtained with models taking into account the actual dimensions of the tyre, the horn effect etc.

The propagation effects are evaluated using the image source method. This method, developed for a simple interface between two semi infinite media has been extended to single and multiple layers in some heuristic way. Although it is now used extensively by many, it will be checked in a further study by comparing it to another method.

The model explains rather well differences in pass-by levels measured over two porous surfaces of similar rolling course and different acoustic absorption.

A numerical correspondence is found between the absorption coefficient in normal incidence and the pass by level difference obtained between a source over the absorbing surface and the source over a reflecting surface. The absorption and attenuation curves in function of frequency have similar shapes but are slightly shifted in frequency.

A numerical law is evaluated for standard pass-by measurement conditions (microphone at 7.5 m distance and 1.2 m height). The law is formulated in 1/3 octave values between the frequency shifted absorption coefficient and the attenuation:

$$\Delta L_p(f_c, 81^\circ) = -11.9 \times \langle a_o(f_{sh.}, 0) \rangle \quad \text{dB}$$

The law is independent of the 1/3 octave frequency.

---

## Bibliography

---

- [1] N-A. Nilsson. Possible methods of reducing external tire noise. In *International tire-noise conference (INTROC)*, Stockholm, 1979.
- [2] W. Liedl. Der einfluss der fahrbahn auf das geräuschprofil von reifen und ein beitrag zu seiner erklärang. l'influence de l'état de la route sur le bruit des pneus lisses et son explication. *Automobil-Industrie*, 22 (3)(3 sept 1977), 1977.
- [3] U. Sandberg and G. Descornet. Road surface influence on tire/road noise - part 1. In *Internoise*, pages 259–272, Miami, 1980.
- [4] Y. Oshino, T. Mikami, H. Ohnishi, and H. Tachibana. Investigation into road vehicle noise reduction by drainage asphalt pavement. *Journal of the Acoustical Society of Japan (E)*, 20(1):75–84, 1999.
- [5] A. von Meier, G.J. van Blokland, and G.G. van Bochove. Reduction of traffic noise by road surface design and tyre-road matching. Technical Report MP.94.1.1, M+P, 1994.
- [6] Kai Ming Li, Tim Waters-Fuller, and K. Attenborough. Sound propagation from a point source over extended reaction ground. *Journal of the Acoustical Society of America*, 104(2) Pt.1(August 1998):679–685, 1998.
- [7] T.F.W. Embleton, J.E. Piercy, and N. Olson. Outdoor sound propagation over ground of finite impedance. *Journal of Acoustical Society of America*, 59(2)(Feb. 1976):267–277, 1975.
- [8] Michael R. Stinson. A note on the use of an approximate formula to predict a sound field above an impedance plane due to a point source. *JASA*, 98(3)(September 1995):1810–1812, 1995.
- [9] J-F. Hamet. Modélisation acoustique d'une chaussée drainante. coefficient d'absorption acoustique en incidence oblique d'un système multicouches. Technical Report N°101, INRETS, 1989.
- [10] J-F. Hamet. Modélisation acoustique d'un enrobé drainant. prise en compte des phénomènes de thermoconductivité dans une nouvelle formulation phénoménologique. Technical Report N°159, INRETS, 1992.
- [11] J-F. Hamet and M. Bérengier. Acoustic characteristics of porous pavements: a new phenomenological model. In *Internoise*, volume II, pages 641–646, Leuven, 1993.
- [12] M-A. Pallas, D. Gaulin, and M. Bérengier. Vertical description of the noise sources of a moving passenger car. In *International conference on sound and vibration*, Garmish-Partenkirchen, 2000.